

1  
2 **Diffuse Ultrasonic Wave-based Structural**  
3 **Health Monitoring for Railway Turnouts**

4  
5  
6 Kai Wang<sup>a</sup>, Wuxiong Cao<sup>a</sup>, Lei Xu<sup>a</sup>, Xiongbing Yang<sup>a</sup>, Zhongqing Su<sup>a,b,c\*</sup>, Xiongjie Zhang<sup>d</sup>,  
7 Lijun Chen<sup>d</sup>

8  
9  
10 <sup>a</sup> Department of Mechanical Engineering

11 The Hong Kong Polytechnic University, Kowloon, Hong Kong SAR

12  
13 <sup>b</sup> National Rail Transit Electrification and Automation Engineering Technology Research  
14 Center (Hong Kong Branch), The Hong Kong Polytechnic University, Kowloon,  
15 Hong Kong SAR

16  
17 <sup>c</sup> The Hong Kong Polytechnic University Shenzhen Research Institute  
18 Shenzhen 518057, P.R. China

19  
20 <sup>d</sup> Southwest Jiaotong University Railway Development Co., Ltd.  
21 Chengdu, 610073, P.R. China

22  
23 **Submitted to *Ultrasonics***

24 (initial submission on 10 August 2019; Revised and re-submitted on 9 September 2019)

25  
26  
27  

---

\* To whom correspondence should be addressed. Tel.: +852-2766-7818, Fax: +852-2365-4703;  
Email: [Zhongqing.Su@polyu.edu.hk](mailto:Zhongqing.Su@polyu.edu.hk) (Prof. Zhongqing SU, *Ph.D.*)

28 **Abstract**

29 Real-time damage evaluation is a critical step to warrant the integrity of turnout systems in  
30 railway industry. Nevertheless, existing structural health monitoring (SHM) approaches,  
31 despite their proven effectiveness in laboratory demonstration, are restricted from *in-situ*  
32 implementation in engineering practice. Based upon the continued endeavors of the authors  
33 in developing SHM approaches and exploring real world applications, an *in-situ* SHM  
34 approach, exploiting active diffuse ultrasonic waves (DUW) and a benchmark-less method,  
35 has been developed and implemented in a marshalling station in China. When trains passing  
36 a railway turnout, the train-induced loads on the rail track can lead to the growth of defects  
37 in the rail, and such growth disturbs the ultrasound traversing at the defect and gives rise to  
38 discrepancies between the DUW signals acquired before and after the train's passage. On  
39 this basis, a damage index, making use of the defect growth-induced changes in DUW  
40 signals, is proposed to identify the presence of defect. The probability of defect growth  
41 induced by the train-related load can be used to assess the severity of the defect. Via an  
42 online diagnosis system, conformance tests are implemented in Chengdu North Marshalling  
43 Station, in which defects in switch rails are identified and the health status of in-service rail  
44 tracks are continuously monitored. The results have demonstrated the effectiveness and  
45 reliability of DUW-driven SHM towards real world railway turnout applications.

46

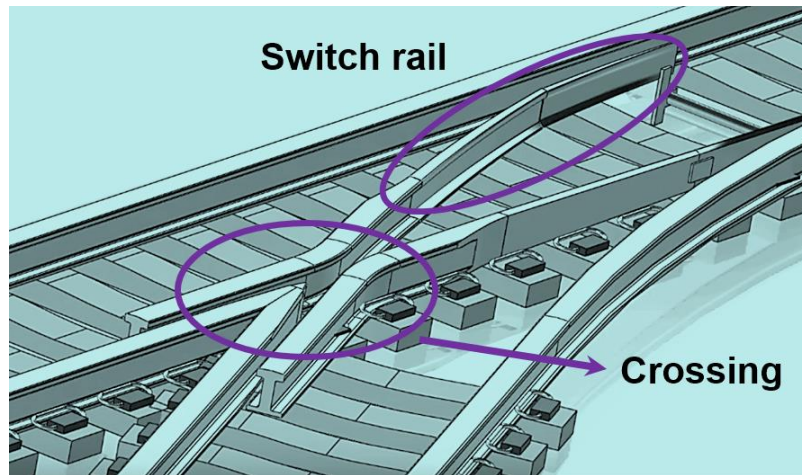
47 **Keywords :** diffuse ultrasonic waves; *in-situ* health monitoring; PZT sensor network;  
48 industrial implementation; railway turnouts

49

## 50 **1. Introduction**

51 With intense use, heavy loads, and harsh environmental conditions, the integrity of rail tracks  
52 has been a paramount concern in railway industry, and this concern is particularly  
53 accentuated for turnout systems. As critical components of railway infrastructure, turnout  
54 systems are used to guide a train to other directions or other tracks. Unlike stock rails, a  
55 turnout system assembles diverse components including switches, crossings, insulators,  
56 fasteners, stock rails, etc. Considering the irregularity of the structure, the turnout system is  
57 more prone to the initiation and propagation of fatigue damage than stock rails in the railway  
58 network, as typified by the switch rail, see **Fig. 1**, because their geometrical features  
59 engender stress concentration in local regions[1]. Furthermore, the discontinuity in the  
60 wheel/rail running surface (the contact patch) is usually remarkable, as shown in **Fig. 1**, and  
61 the wheel/rail interaction at this imperfect contact leads to the generation of intense impact  
62 loads[2] that severely jeopardize the health of the rails. Taking the impact load-induced  
63 damage and the fatigue damage induced by passing trains and thermal variation into  
64 consideration, defects in railway turnouts can be developed and lead to catastrophic disasters.  
65 As reported elsewhere[3], turnout component failures account for the vast majority of  
66 derailments. As an example, a derailment occurred near Hilversum station on 15 January  
67 2014, and subsequent investigation showed that a fatigue fracture in the ring of the switch,  
68 owing to overdue switch maintenance, was the culprit.

69



70  
71 **Fig. 1.** Turnout system comprising switch and crossing  
72

73 With integrity a paramount concern for railway turnouts, a number of non-destructive  
74 evaluation (NDE) methods have been advocated for inspection of rail defects. Prevailing  
75 NDE techniques that are readily available for rail maintenance are represented by those using  
76 eddy current[4, 5], visual cameras[6], magnetic testing[7], and ultrasonic inspection[8-11],  
77 to name a few. Among these techniques, the ultrasonic inspection-based technique is the  
78 most prevalently applied, with the aid of which routine inspection and maintenance has been  
79 conducted. Despite their merits in perceiving gross damage, with a nature of off-line  
80 manipulation and a high degree of human interaction, most of the aforementioned NDE  
81 approaches are inherently unwieldy for timely awareness of rail defects and continuous  
82 monitoring of deterioration. Implemented at scheduled intervals after normal service of an  
83 inspected railway has been terminated, they are costly, time-consuming, and labor-intensive.  
84 Most importantly, when applied to the inspection of the turnout system, these ultrasonic  
85 inspection-based techniques are infeasible because they cannot provide efficient access to  
86 parts of the turnout system, due to the irregular structure at the turnout system, such as the  
87 switch rail as displayed in **Fig. 1**.

88  
89 To circumvent the deficiencies described, structural health monitoring (SHM) tailor-made

90 for rail tracks emerges to warrant continuous/real-time and automated surveillance of the  
91 integrity of rail tracks. In this regard, acoustic emission (AE)-based SHM methods[12-17]  
92 that passively utilize the abrupt energy release when a crack grows have proven their  
93 effectiveness. Although a number of AE-based techniques have been reported, this group of  
94 techniques is demonstrably effective only in laboratory environments. When applied in  
95 engineering practice, they are principally confronted with a twofold bottleneck: (1) the  
96 acoustic signals caused by various practical factors such as wheel/rail interaction, impact  
97 load, and wheel/rail creep are usually overwhelming, and therefore the damaged-related AE  
98 can be obfuscated or masked; (2) when dealing with damage that grows at a low rate (e.g.  
99 imperceptible fatigue crack growth or low load-induced growth), AE-based approaches may  
100 lose their effectiveness – because such damage growth would not lead to a notable energy  
101 release, and this will result in the deficiency stated in (1). Although researchers have  
102 exhaustively attempted to discern the damage-related signals from the noise, even with the  
103 aid of powerful artificial intelligence methods [14], this group of techniques often shows  
104 unsatisfactory performance in engineering practice, in terms of their fidelity, reliability,  
105 adaptability, and environment tolerance.

106

107 To tackle the deficiencies of passive AE-based methods, SHM approaches using active  
108 guided ultrasonic waves (GUWs) in rails are attracting increasing research efforts[18-27].  
109 The effectiveness of this category of approaches lies in the premise that defects in the rail  
110 disturb the propagation of inspecting waves and, by evaluating the changes in wave  
111 propagation features, defects can be identified. Nevertheless, when extended to rail tracks,  
112 particularly the turnout system, these approaches that utilize specific wave modes lose  
113 effectiveness because of the perplexing wave scattering/reflections at irregular boundaries,  
114 high complexity of wave propagation as a result of multimodal and dispersive features (e.g.,

115 GUWs, longitudinal waves, surface waves) and modes overlapping. Therefore, it is  
116 challenging to isolate and extract damaged-associated features using existing GUWs-based  
117 methods, precluding their application in SHM for railway turnout systems.

118

119 To provide continuous and automated surveillance of structural health conditions without  
120 suspending the normal operation of the railway turnout system, an active approach based on  
121 diffuse ultrasonic waves (DUWs) is developed in this study. In this approach, the rail track  
122 is treated as a diffusive medium in which incident acoustic wave energy is rapidly  
123 reverberated, resulting in a diffuse ultrasonic wave field that encompasses multiple wave  
124 modes such as GUWs, longitudinal waves, and surfaces waves. Despite its complex  
125 appearance, the DUW features high repeatability and is sensitive even to subtle change in  
126 material or structural properties [28-30]. Via processing DUWs as a whole, instead of  
127 isolating and discerning specific wave modes, the health condition of the railway turnout  
128 system can be evaluated holistically.

129

130 On this basis, damage indices that calibrate the health condition of rail tracks can be  
131 constructed by making use of the features of DUWs. To this end, a benchmark-less method  
132 is proposed. In this method, the presence of a defect is identified via the effect of newly  
133 growing defect, rather than the existing defect, on the propagation of DUWs. This method  
134 exploits the contrast between DUWs acquired before and after a train passage, rather than  
135 using contrast against an outdated baseline, and this leads to enhancement of the precision  
136 and the robustness of defect detection. The proposed DUW-driven approach is deployed and  
137 implemented on a railway turnout in a marshalling station in China via a previously  
138 developed online diagnosis system. To prove the effectiveness and reliability of the proposed  
139 approach, rail tracks bearing a defect are examined and health monitoring of intact, in-

140 service rail tracks is performed. Using integrated sensors, pre-developed devices, and proper  
141 signal processing techniques, the proposed DUW-driven SHM approach is capable of  
142 enhancing the safety of turnout systems in a robust and economic fashion.

143

## 144 **2. Methodology**

### 145 ***2.1. DUWs in railway track***

146 Considering the complex geometrical manifestation of rail track and the practical constraints  
147 on instrument installation, the incident waves are multimodal which are multi-scattered by  
148 boundaries. Therefore, the acoustic energy is rapidly reverberated and adequately  
149 disseminated throughout the entire rail track section (see **Fig. 2**). In this context, although  
150 the material properties of the rail track are distinct from those of diffusive medium such as  
151 concrete, the rail track can be deemed a one-dimensional diffusive medium along the train's  
152 running direction. In this one-dimensional diffusive medium, the DUWs propagating in the  
153 rail track are extremely sophisticated, owing to the fact that multiple wave modes coexist,  
154 including bulk waves, surface waves, and GUWs, and they are intricately overlapped and  
155 intertwined. It is fairly challenging therefore, to isolate and discern each wave mode from  
156 such a complex DUW waveform. With this backdrop, the DUWs in the inspected rail section  
157 are treated as a whole and processed holistically to extract features that are capable of  
158 identifying and characterizing defects in the rail.

159

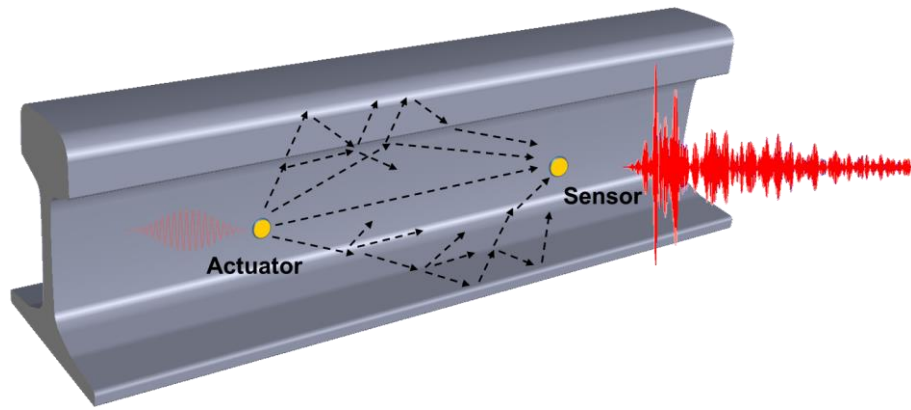


**Fig. 2.** DUWs in a rail after multi-scattering and mode conversions

160

161

162

163 In conventional methods, a benchmark process against baseline signals that highlights  
 164 defect-related changes in wave signals is required to characterize the defect, and the baseline  
 165 signals are pre-collected from an intact specimen under given conditions [31-33]. Although  
 166 this method is effective in principle, the detection philosophy is prone to contamination from  
 167 noise introduced by diverse practical factors. Typically, wave signal acquisition can be  
 168 influenced significantly by factors such as instrument error, system malfunction, condition  
 169 variation, and atrocious climate. These practical factors can lead to baseline drift even  
 170 without the presence of defect, and this drift is often overwhelming above defect-associated  
 171 changes in DUW signals. As a result, false-positive alarms can be produced, and existing  
 172 defects can be obscured. With this backdrop, a benchmark-less method is proposed to isolate  
 173 defect-associated changes in DUWs, enhancing the robustness and reliability of health  
 174 condition evaluation using DUWs.

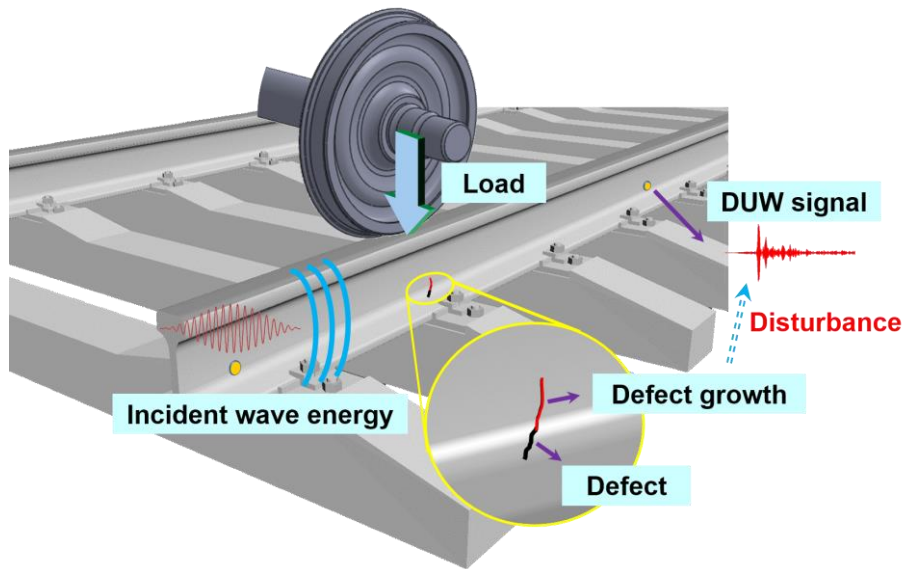
175

## 176 ***2.2. Benchmark-less evaluation method using DUWs***

177 To circumvent the interference linked with diverse practical factors, a pair of DUW signals  
 178 from an inspected rail turnout, which are respectively acquired before and after the passage  
 179 of a train, are contrasted. The passing train exerts a load on the rail track, and if any defect  
 180 exists, such as a fatigue crack, the load exerted by the passing train can lead to the growth of



181 the defect. This defect growth induces disturbance in the DUWs traversing at the defect,  
 182 thereby producing a remarkable deviation of the DUWs after the train passage from those  
 183 ascertained before the train passage, as illustrated schematically in Fig. 3. Usually, the  
 184 passing of a train takes only a short period (e.g. less than a few minutes), during which the  
 185 service conditions, the system, and the instrument are invariant. Therefore, interference  
 186 induced by those practical factors is negligible. In this context, changes in the pair of DUW  
 187 signals are linked with the defect alone and, if no defect exists in the inspected turnout, the  
 188 variation between the pair of DUW signals is insidious.  
 189



190

191 **Fig. 3.** Load induced by passage of train leads to defect growth causing disturbance in  
 192 DUWs

193

194 On this basis, to assess the variations in DUWs induced by growth of a defect, a damage  
 195 index is defined that calibrates the level of decorrelation between the pair of DUW signals  
 196 and reads

197

$$R_{cc} = 1 - \frac{\int X(t)Y(t)dt}{\sqrt{\int X(t)^2 dt \int Y(t)^2 dt}}. \quad (1)$$

198 In Eq. (1),  $X(t)$  and  $Y(t)$  denote the DUW signals acquired before and after the passage  
199 of a train, respectively.  $R_{cc}$  denotes the remnant cross correlation. It is envisioned that the  
200 more severe the defect in the rail turnout, the greater will be the growth of the defect when  
201 subjected to a train passage induced-load, producing a higher  $R_{cc}$ .

202

203 It is worth noting that the probability of defect growth increases with its severity. Therefore,  
204 the proposed  $R_{cc}$  can be used to identify the presence of a defect and to evaluate its  
205 severity in a quantitative manner. This method can alleviate dependence on the baseline,  
206 thereby enhancing the environment tolerance, adaptability, and robustness of health  
207 condition evaluation, providing the basis for application in reality.

208

### 209 **3. Implementation of SHM on turnout in a marshalling station**

#### 210 ***3.1. System set-up***

211 To implement the developed SHM approach, an integrated online diagnosis system[19]  
212 previously designed by the authors is exploited, which is developed on a PCI extension for  
213 instrumentation (PXI) platform with the virtual instrument technique. Through the PXI bus  
214 and in-house software, the compact system embraces modules including an arbitrary wave  
215 generation module, a multi-channel data acquisition module, and a central control and data  
216 processing module[34]. In conjunction with the use of an active sensor network, the  
217 diagnosis system is capable of performing automatic and online surveillance of the health  
218 condition of a rail turnout. For the sensor installation on the rail turnout, lead zirconate  
219 titanate (PZT) wafers are appropriate for the practical application (see **Fig. 4**), owing to  
220 several advantageous features: substantial weight saving over conventional ultrasonic  
221 actuating and sensing devices, negligible footprint, ease of integration into host structures,

222 high operating frequency, dual roles as actuator and sensor, as well as low cost.

223



224

225 **Fig. 4.** Online diagnosis system and the PZT wafers used to construct sensor network  
226

227 Owing to the holistic monitoring capability of the DUW-based method, a sparse sensor  
228 network consisting of two PZT wafers is sufficient to enable DUW excitation and acquisition  
229 in a rail turnout, realizing implementation of the developed approach in an economical and  
230 convenient fashion. The positioning of PZT wafers does not entail exhaustively prudent  
231 selection, thus providing an effortless and universal solution to DUW excitation and  
232 acquisition in rail turnout systems with different designs, in which the geometry of the  
233 turnout system can vary remarkably.

234

### 235 **3.2. In-situ SHM of railway turnout in marshalling station**

236 The developed SHM technique, deployed via the online diagnosis system, was installed on  
237 the turnout system in the Chengdu North Marshalling Station in China in December 2018,  
238 for *in-situ* monitoring of the health condition of the turnout system.

239

240 The Chengdu North Marshalling Station, as photographed in **Fig. 5**, is the largest freight  
241 classification yard in Southwest China, featuring a hump and over 100 tracks. In this station,

242 around 10,000 freight trains consisting of isolated cars with a combined weight of more than  
243 90 million tons are separated, classified, and made into trains according to their destinations  
244 every day. In the classification process, the cars are shunted several times along their route  
245 through turnout systems, as photographed in **Fig. 6**. Such frequent passing of heavy freight  
246 trains exerts intense loads on the turnout systems. In addition to the intense load induced by  
247 trains, they are also exposed to a wide array of hazards such as detrimental impacts, atrocious  
248 climate, complex rail conditions, and unexpected events. Therefore, the turnout systems are  
249 highly prone to structural damage, and a number of damaged rail tracks in the turnout  
250 systems are produced every year.



251

252

**Fig. 5.** Chengdu North Marshalling Station



253

254

**Fig. 6.** The hump and the turnout systems in the marshalling station

255

256 To implement the developed SHM approach on the selected turnout system, a pair of PZT  
257 wafers (PI<sup>®</sup>, P51, diameter: 12 mm and thickness: 1 mm) were surface-mounted on the rail  
258 track prior to the conformance testing. Considering practical constraints, the PZT wafers  
259 were located at the rail web at a distance of 70 mm from the rail bottom. The sensor network  
260 was then connected to the online diagnosis system, which was accessible to an operator. *In-*  
261 *situ* SHM was performed in the manner of periodic scans. In the DUW test, five-cycle  
262 sinusoidal tone bursts modulated by a Hanning window were generated by the waveform  
263 generation module at a central frequency of 250 kHz at which strongest responses can be  
264 obtained, and the collected data from 128 consecutive scans were averaged so as to increase  
265 the signal/noise ratio. Given a propagation speed of  $\sim 5$  km/s of the longitudinal waves in  
266 steel, the ultrasonic energy could be diffused sufficiently within a time span of 10 ms for a  
267 rail with length up to 10 m. Therefore, the DUWs in 10 ms were collected with the PZT  
268 wafers at a sampling rate of 25 MHz through the data acquisition module, to encompass  
269 desirably rich information pertaining to the status of the overall rail track.

270

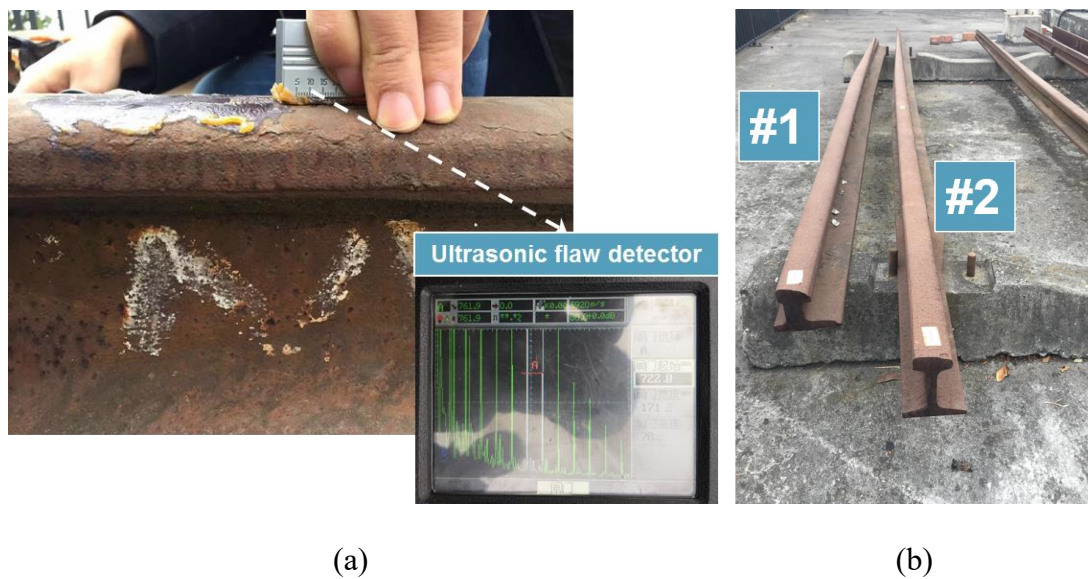
271 To comprehensively evaluate the developed approach and the online diagnosis system, both  
272 the damaged rail tracks and in-service rail tracks were examined.

273

### 274 ***3.3. Application on damaged rail track***

275 To validate the detection capability of the proposed method, damaged rail tracks dismantled  
276 from the turnout system in the marshalling station were first examined. As already explained,  
277 the switch rail is usually subjected to the impact force owing to the passage of the train,  
278 leading to the initiation and evolution of fatigue damage. **With an ultrasonic flaw detector**  
279 **maneuvered by an operator, the fatigue damage can be detected. The ultrasonic flaw detector**  
280 **which emits probing ultrasonic waves into the rail and acquires the reflected waves scans**

281 along the surface of rail head. At the section in which a defect exists, strong reflection can  
282 be detected, as shown in Fig. 7(a), and ignorable reflection is generated in intact regions.  
283 Once damage is identified and confirmed, the damaged rail track is immediately replaced by  
284 an intact track. Fig. 7(b) displays damaged rail tracks, denoted #1 and #2, that were  
285 disassembled from the marshalling station and measured 4.5 m and 5.5 m in length  
286 respectively.



287  
288  
289  
290  
291

**Fig. 7.** (a) Damage detection using ultrasonic flaw detector; (b) damaged switch rails from the Chengdu North Marshalling Station

292 A pair of PZT wafers was surface-mounted on the rail track. For illustration, a photograph  
293 of the rail with integrated sensors is shown in Fig. 8. The PZT wafers (denoted by PZT1 and  
294 PZT2) were positioned 3 m apart. To instigate load-induced defect growth, a hydraulic press  
295 was used to apply a load of 100 kN, as displayed in Fig. 8, which was consistent with the  
296 load exerted by a passing train in the marshalling station. DUWs were excited and acquired  
297 using the PZT wafer-based sensor network before application of the load and after removal  
298 of the load. This DUW test was repeated 15 times on each rail track.

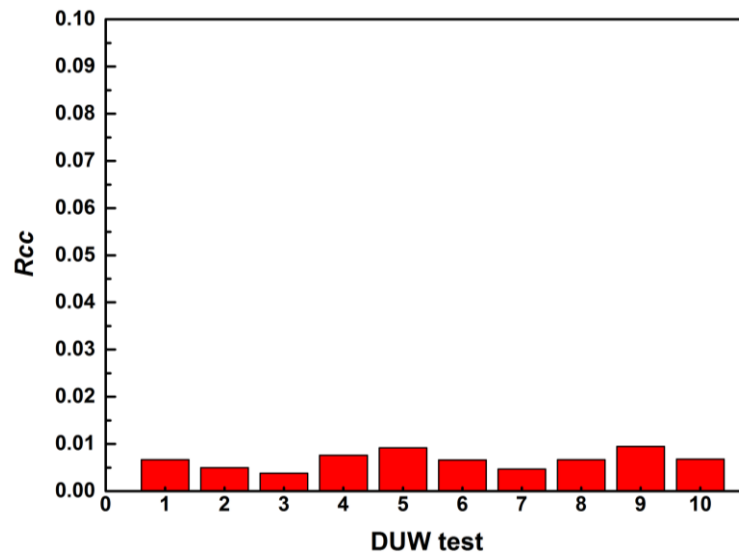


299

300 **Fig. 8.** The hydraulic press used to exert load on the rail and the sensor network on the web  
 301 of the rail

302

303 With the DUW signals acquired in each DUW test, the defined damage index could be  
 304 constructed with Eq. (1). From the authors' previous research, it is concluded that in an intact  
 305 rail track, the load induces no defect growth, and the signals ascertained before and after the  
 306 load are almost invariant. Fig. 9 displays the damage index obtained using the DUW signals  
 307 from the tests in intact rail tracks which are performed using the same set-up and repeated  
 308 10 times. It is clearly demonstrated that the proposed damage index is not greater than 1%.  
 309 With this background, a threshold (1%) for the damage index  $R_{cc}$  was proposed, and  
 310 defect growth was deemed to have occurred when the threshold was reached.



311 **Fig. 9.** The damage indices  $R_{cc}$  from each DUW test on intact rail  
 312  
 313

314 **Fig. 10** (a) and (b) representatively display the DUWs from two DUW tests on #1 rail. In

315 **Fig. 10(a)**, a remarkable difference is clearly demonstrated between the signals acquired  
 316 before and after the load, whereas no discernable change is exhibited in the signals shown  
 317 in **Fig. 10(b)**. It is worth noting that the crack growth is in nature a local event, and thus only

318 the propagation of certain wave modes that traverse at the crack is alternated. As a result, the  
 319 acquired signals in certain time windows are changed, as displayed in the inset in **Fig. 10(a)**.

320 Using Eq. (1), the damage indices  $R_{cc}$  in each DUW test are ascertained and displayed in

321 **Fig. 11** for #1 rail and **Fig. 12** for #2 rail. It is clear that in the DUW tests denoted by 1, 4,  
 322 and 11 for #1 rail and those denoted by 3 and 9 for #2 rail, a remarkable increase in  $R_{cc}$

323 is generated, whereas in other tests the  $R_{cc}$  are lower than the threshold. These phenomena

324 indicate that in these tests (1, 4, 11 for #1 rail and 3, 9 for #2 rail) the defect growth that leads

325 to disturbance in the probing DUW is induced by the load. To verify the defect growth, the

326 ultrasonic flaw detector is used to measure the amplitude of reflection of probing ultrasonic

327 waves in #1 rail, and the increasing in amplitude of the reflection induced by each exertion

328 of the load is obtained. It is clearly demonstrated that remarkable increasing is only detected

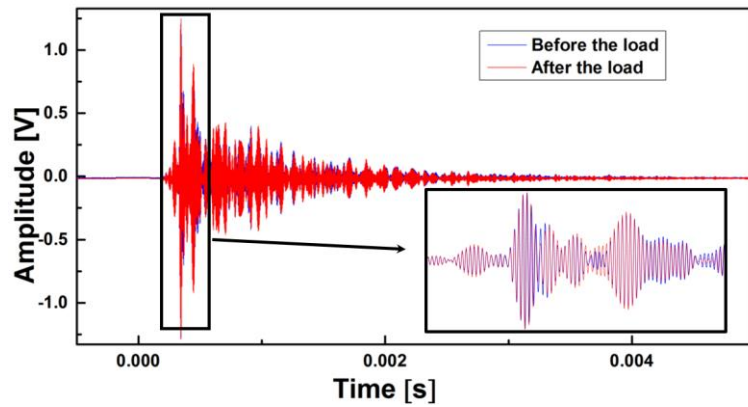
329 in the DUW tests denoted by 1, 4, 11 for #1 rail, corroborating with the evaluation results



330 using the proposed approach.

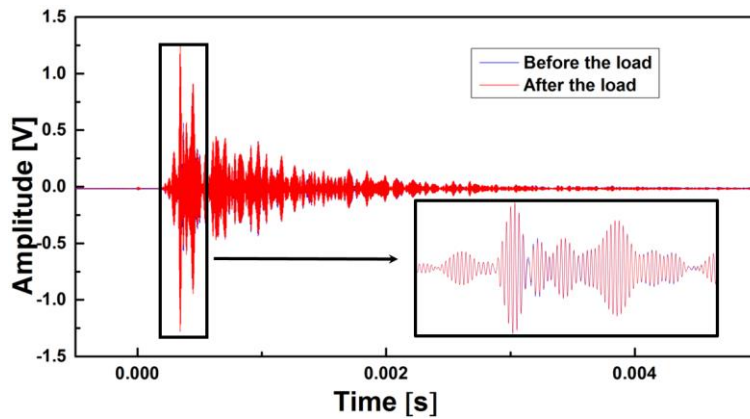
331

332 Taking a step further, among 15 DUW tests, defect propagation is identified in three tests for  
333 #1 rail and two tests for #2 rail. These results assert that, compared with the scenario in  
334 which the defect is of small scale and the probability of defect growth is low (usually lower  
335 than 1%), the probability of defect growth under the load is high. Therefore, it can be  
336 concluded that a severe defect exists in both inspected switch rails.



337  
338

(a)



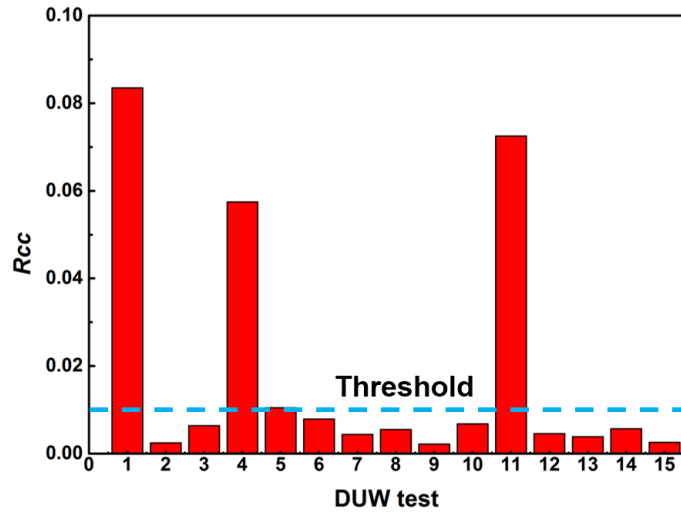
339

340

(b)

341 **Fig. 10.** The DUW signals in scenarios: (a) when defect growth occurs and (b) when no  
342 defect growth occurs

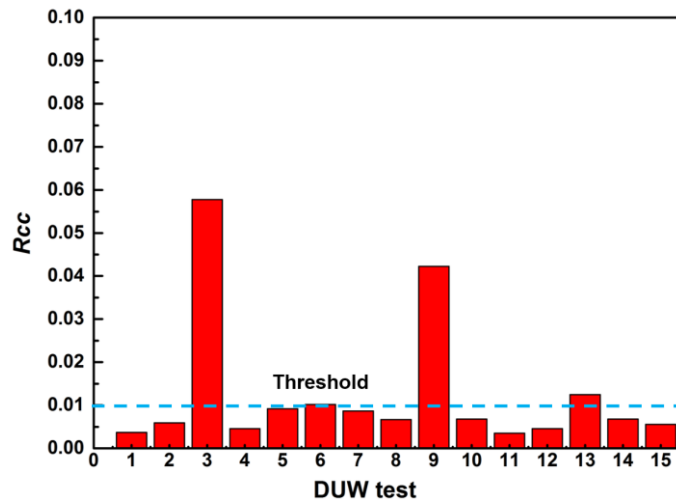
343



344

345 **Fig. 11.** The damage indices  $R_{cc}$  from each DUW test on #1 rail

346



347

348 **Fig. 12.** The damage indices  $R_{cc}$  from each DUW test on #2 rail

349

350

It is worth noting that in reality the load applied on the railway track is caused by moving

351

trains with low frequency vibration. Considering that the proposed method identifies the

352

fatigue damage in the rail track by assessing the load-induced damage growth, and features

353

of the load (static load or low-frequency cyclic load) impose insignificant influence on DUW

354

signals acquired before the load and after the removal of the load. Therefore, despite that the

355

static load applied in the experiment is different from the load induced by moving trains in

356

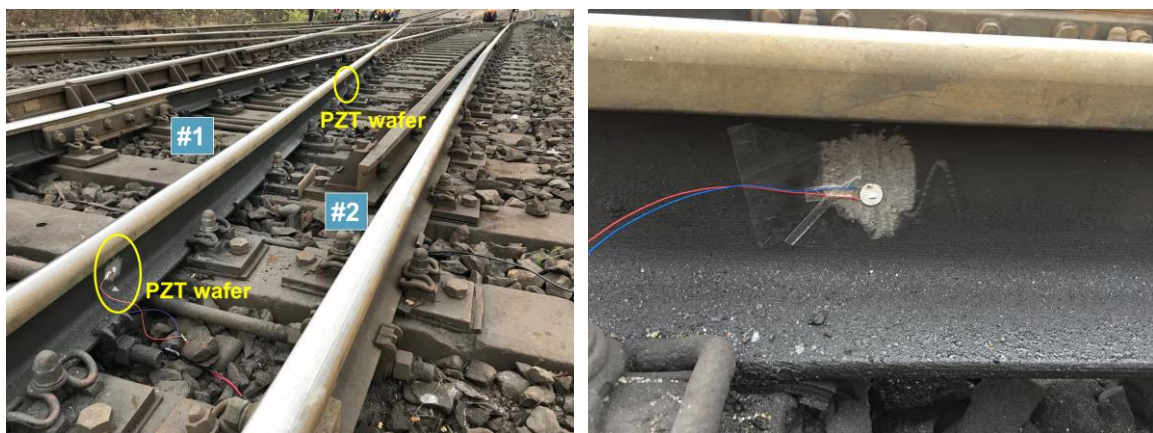
reality, the evaluation of crack growth is not influenced by the load type.

357

358 **3.4. Application on in-service rail track**

359 To examine the reliability and robustness of the developed SHM technique, *in-situ*  
360 monitoring for the health condition of in-service rail tracks in a turnout system was  
361 performed. Two rail tracks in a turnout system were selected as the monitoring object,  
362 denoted by #1 and #2. During the suspension window period of the marshalling station, a  
363 pair of PZT wafers was installed 5 m apart on the web of each track, as demonstrated in **Fig.**  
364 **13**, to excite and acquire DUWs in the rail. This pair of PZT wafers was then connected with  
365 the diagnosis system (see **Fig. 14**). Load exerted on the rail by a passing train can lead to the  
366 growth of a defect, if any, in the rail. By evaluating the train-induced defect growth, the  
367 health condition of the monitored rail track can be assessed using the developed SHM  
368 method.

369



370

371

372

373

**Fig. 13.** The sensor network installed on the turnout system



374

375

376 **Fig. 14.** The online diagnosis system used for the *in-situ* health monitoring of in-service  
377 rail track

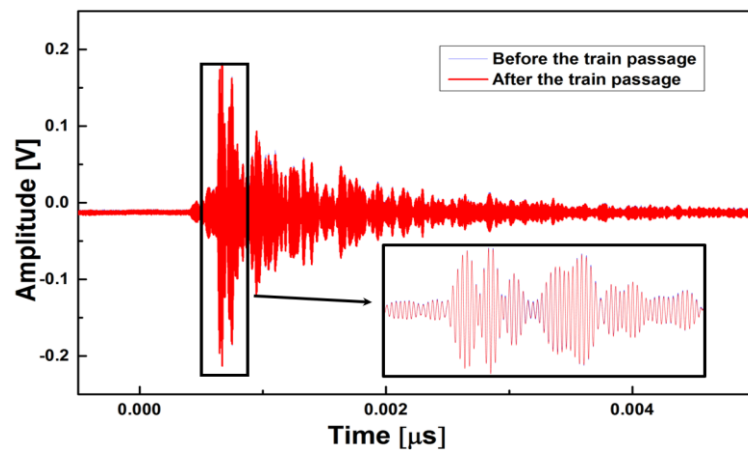
378

379 The DUW signals were acquired before and after the passing of a train and, in conjunction  
380 with Eq. (1), the proposed damage index  $R_{cc}$  was ascertained. **Fig. 15(a)** displays the  
381 DUWs from #1 rail acquired before and after the passing of a freight train weighing 96 t,  
382 and the damage index obtained using Eq. (1) is 2.8%. **Fig. 16(a)** displays the representative  
383 DUWs from #2 rail. The damage indices in 15 DUW tests are exhibited in **Fig. 15(b)** for #1  
384 rail and **Fig. 16(b)** for #2 rail, from which it is observed that no remarkable increase in  $R_{cc}$   
385 is generated in these tests. Therefore, it can be concluded the rail tracks in-service were in  
386 an intact status. It is worth noting that the conformation tests were performed on a rainy day  
387 in winter when the temperature was below  $5^{\circ}\text{C}$  and the humidity was high. Despite these  
388 harsh climate conditions, the evaluation results exhibited the effectiveness and reliability of  
389 the proposed approach, proving its environmental adaptability.

390

391 It is also worth noting that, although the monitored rail track was in an intact status, the  
392 damage index was slightly greater than the pre-set threshold (1%). As demonstrated in **Fig.**  
393 **15** and **Fig. 16**, the maximum of the damage index for #1 rail is 3% and that for #2 rail is

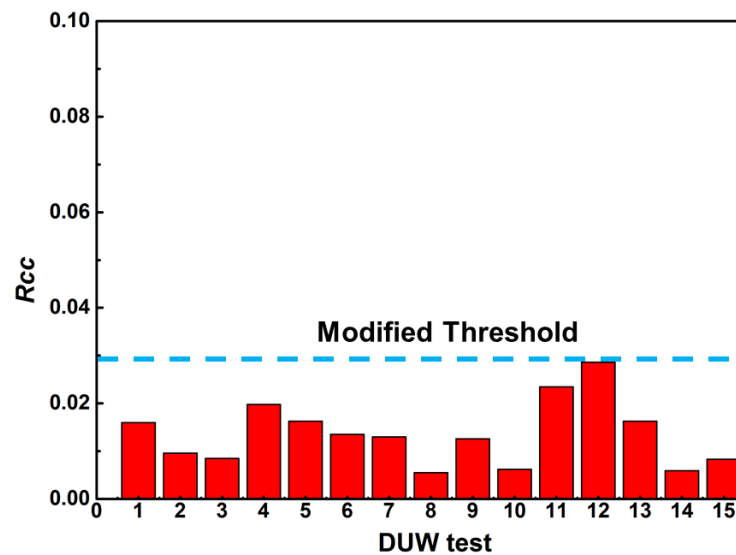
394 2.5%. This is because the train passage leads to changes in the rail structures, such as the rail  
 395 fastening, which impose an influence on the DUWs in the rail track, and therefore, the  
 396 damage index is increased. This result implies that, in a practical application, a modified  
 397 threshold (e.g. 3%), as exhibited in **Fig. 15** (b) and **Fig. 16**(b), that can be acquired  
 398 empirically is required to obtain a reliable evaluation of health condition.  
 399



400

401

(a)



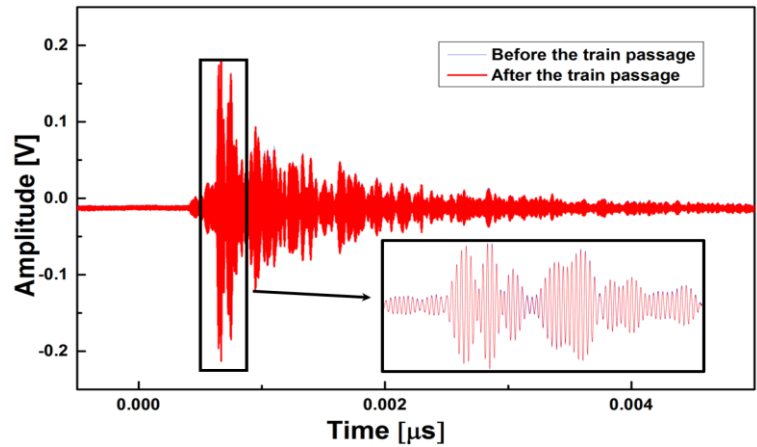
402

403

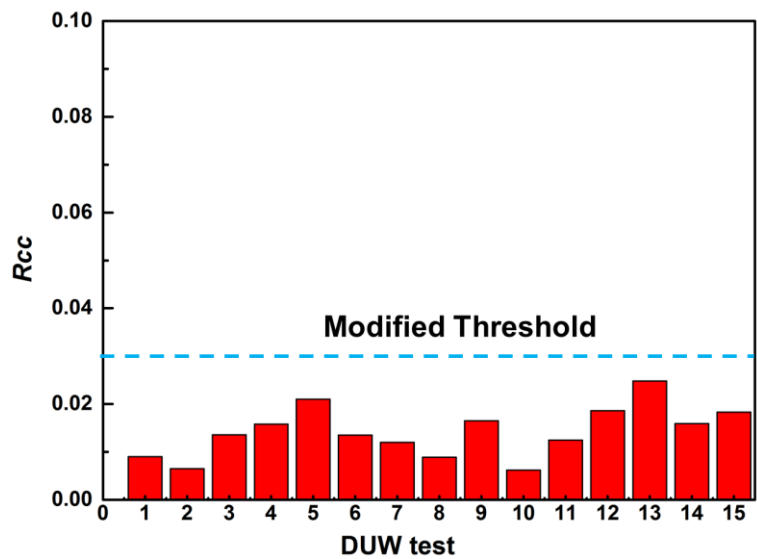
(b)

404 **Fig. 15.** (a) The signals in a DUW test and (b) the damage indices  $R_{cc}$  from each DUW  
 405 test on #1 in-service rail

406



(a)



(b)

**Fig. 16.** (a) The signals in a DUW test and (b) the damage indices  $R_{cc}$  from each DUW test on #2 in-service rail

407

408

409

410

411

412

413

414

415

416

417

418

419

420

421

422

The proposed benchmark-less method using DUWs can fulfill *in-situ* health monitoring of the rail track in an online manner. This method is capable of identifying the crack growth induced by each train passage and, via assessing the probability of growth of the defect, can evaluate the severity of the defect. It is also worth pointing out that, provided the influence of practical factors on the DUW testing is consistent over a certain period (e.g. a few weeks), the accumulated growth of a defect in this period that encompasses multiple train passages can be evaluated using the proposed method. Thus, a defect can be identified and evaluated

423 even when the individual crack growth induced by train passage is minimal, such that the  
424 AE energy is so weak that it cannot be detected using an existing AE-based method.  
425 Moreover, compared with widely studied AE methods, the proposed method features higher  
426 reliability because typical AE methods evaluate cracks via their sudden growth which is an  
427 instantly occurring event, whereas the proposed method is based on assessment of defect  
428 growth that can be performed repeatedly. In addition, the developed method can be readily  
429 applied to the monitoring of different rail types and to inaccessible sections of rail by  
430 appropriate distribution of PZT wafers (e.g. pitch-catch or pulse-echo configuration). For  
431 example, for a switch rail, at the tip of which the installation of an instrument is strictly  
432 prohibited, two PZT wafers installed at a certain distance from the tip, forming a pulse-echo  
433 configuration, can be exploited to implement the developed monitoring approach. It is also  
434 worth noting that the effectiveness of the proposed approach lies in the fact that the defect is  
435 detected by assessing its growth when the rail is subjected to external load, and thus the  
436 developed approach can also be used to detect defects of diverse types, for example the  
437 pitting corrosion, that can expand due to external load and induce changes in DUWs.

438

439 Given the appealing merits of the diffuse features of DUWs, this method is capable of  
440 monitoring the overall health of the turnout system using a sparse sensor network and does  
441 not entail an exhaustively prudent selection of sensor position. The distance of the adjacent  
442 PZT transducers is mainly dependent on the amplitude of DUW signals, and using the above  
443 set-up, a pair of PZT transducers can be exploited for the effective and reliable monitoring  
444 of rail tracks measuring 8m in length. Thus the method can accommodate practical  
445 restrictions in terms of weight, volume, and mounting manner. Most importantly, the  
446 utilization of benchmark-less concept in the proposed method alleviates dependence on  
447 baseline signals obtained from an intact specimen, thereby rendering immunity to

448 interference induced by various practical factors, warranting the performance of the system  
449 in different service conditions. This enhancement of robustness improves the readiness level  
450 of the proposed method, benefiting its suitability for application in engineering practice.

451

#### 452 **4. Conclusions**

453 Targeting *in-situ* health monitoring of railway turnouts, a benchmark-less method that makes  
454 use of diffuse ultrasonic waves in the rail track is developed in this study. With this method,  
455 diffuse ultrasonic waves are generated and acquired with a sparse sensor network. Wave  
456 signals in a rail track are captured before and after the passage of a train. If defect growth is  
457 induced by the train passage, discrepancies are introduced between the signals obtained  
458 before and after the train passage. By contrasting these signals, a damage index is constructed,  
459 whereby the defect can be identified and evaluated. The proposed method is experimentally  
460 examined via conformance testing, in which the DUW tests are performed on a switch rail  
461 with a defect and an in-service rail turnout from Chengdu North Marshalling Station in China.  
462 Utilizing the proposed method, the defect is identified, and the health condition of the rail  
463 track can be monitored *in-situ* and automatically.

464

465

#### 466 **Acknowledgments**

467 The work was supported by a Key Project (No. 51635008) and a General Project (51875492)  
468 of the National Natural Science Foundation of China. The authors also acknowledge the  
469 support from the Hong Kong Research Grants Council via General Research Fund (Nos.:  
470 15201416 and 15212417) and a research grant from the National Rail Transit Electrification  
471 and Automation Engineering Technology Research Center (No. BBY8).

472



473 **References**

- 474 [1] M. Wiest, W. Daves, F. Fischer, H. Ossberger, Deformation and damage of a  
475 crossing nose due to wheel passages, *Wear*, 265 (2008) 1431-1438.
- 476 [2] S. Kaewunruen, Monitoring structural deterioration of railway turnout systems  
477 via dynamic wheel/rail interaction, *Case Studies in Nondestructive Testing and*  
478 *Evaluation*, 1 (2014) 19-24.
- 479 [3] S. Dindar, S. Kaewunruen, Assessment of turnout-related derailments by various  
480 causes, in: "International Congress and Exhibition" Sustainable Civil  
481 Infrastructures: Innovative Infrastructure Geotechnology", Springer, 2017, pp. 27-  
482 39.
- 483 [4] Z. Song, T. Yamada, H. Shitara, Y. Takemura, Detection of damage and crack in  
484 railhead by using eddy current testing, *Journal of Electromagnetic Analysis and*  
485 *Applications*, 3 (2011) 546.
- 486 [5] J. Rajamäki, M. Vippola, A. Nurmikolu, T. Viitala, Limitations of eddy current  
487 inspection in railway rail evaluation, *Proceedings of the Institution of Mechanical*  
488 *Engineers, Part F: Journal of Rail and Rapid Transit*, 232 (2018) 121-129.
- 489 [6] C. Mair, S. Fararooy, Practice and potential of computer vision for railways,  
490 (1998).
- 491 [7] Z. Liu, W. Li, F. Xue, J. Xiafang, B. Bu, Z. Yi, Electromagnetic tomography rail  
492 defect inspection, *IEEE Trans. Magn.*, 51 (2015) 1-7.
- 493 [8] W. Zhu, Y. Xiang, C.-J. Liu, M. Deng, F.-Z. Xuan, A feasibility study on fatigue  
494 damage evaluation using nonlinear Lamb waves with group-velocity mismatching,  
495 *Ultrasonics*, 90 (2018) 18-22.
- 496 [9] X. Yu, M. Ratassepp, Z. Fan, Damage detection in quasi-isotropic composite  
497 bends using ultrasonic feature guided waves, *Compos. Sci. Technol.*, 141 (2017)  
498 120-129.
- 499 [10] J. Rao, M. Ratassepp, Z. Fan, Guided wave tomography based on full waveform  
500 inversion, *IEEE Trans. Ultrason. Ferroelectr. Freq. Control*, 63 (2016) 737-745.
- 501 [11] L.T. Nguyen, R.T. Modrak, Ultrasonic wavefield inversion and migration in  
502 complex heterogeneous structures: 2D numerical imaging and nondestructive  
503 testing experiments, *Ultrasonics*, 82 (2018) 357-370.
- 504 [12] K. Bruzelius, D. Mba, An initial investigation on the potential applicability of  
505 Acoustic Emission to rail track fault detection, *NDT & E Int.*, 37 (2004) 507-516.
- 506 [13] N. Thakkar, J. Steel, R. Reuben, Rail-wheel interaction monitoring using  
507 Acoustic Emission: A laboratory study of normal rolling signals with natural rail  
508 defects, *Mech. Syst. Signal Process*, 24 (2010) 256-266.
- 509 [14] J. Wang, X.Z. Liu, Y.Q. Ni, A Bayesian Probabilistic Approach for Acoustic  
510 Emission-Based Rail Condition Assessment, *Computer-Aided Civil and*  
511 *Infrastructure Engineering*, 33 (2018) 21-34.
- 512 [15] L. Qiu, B. Liu, S. Yuan, Z. Su, Impact imaging of aircraft composite structure  
513 based on a model-independent spatial-wavenumber filter, *Ultrasonics*, 64 (2016)  
514 10-24.
- 515 [16] K. Wang, Y. Li, Z. Su, R. Guan, Y. Lu, S. Yuan, Nonlinear aspects of "breathing"

- 516 crack-disturbed plate waves: 3-D analytical modeling with experimental  
517 validation, *Int. J. Mech. Sci.*, 159 (2019) 140-150.
- 518 [17] N. Nazeer, M. Ratssepp, Z. Fan, Damage detection in bent plates using shear  
519 horizontal guided waves, *Ultrasonics*, 75 (2017) 155-163.
- 520 [18] Z. Su, C. Zhou, M. Hong, L. Cheng, Q. Wang, X. Qing, Acousto-ultrasonics-based  
521 fatigue damage characterization: Linear versus nonlinear signal features, *Mech.*  
522 *Syst. Signal Process*, 45 (2014) 225-239.
- 523 [19] M. Hong, Q. Wang, Z. Su, L. Cheng, In situ health monitoring for bogie systems  
524 of CRH380 train on Beijing–Shanghai high-speed railway, *Mech. Syst. Signal*  
525 *Process*, 45 (2014) 378-395.
- 526 [20] P. Cawley, P. Wilcox, D. Alleyne, B. Pavlakovic, M. Evans, K. Vine, M.J. Lowe,  
527 Long range inspection of rail using guided waves-field experience, in:  
528 *Proceedings of the 16th World Conference on Non-Destructive Testing*, Montreal,  
529 Canada, Citeseer, 2004.
- 530 [21] F. Lanza di Scalea, P. Rizzo, S. Coccia, I. Bartoli, M. Fateh, E. Viola, G. Pascale,  
531 Non-contact ultrasonic inspection of rails and signal processing for automatic  
532 defect detection and classification, *Insight-Non-Destructive Testing and Condition*  
533 *Monitoring*, 47 (2005) 346-353.
- 534 [22] L. Qiu, S. Yuan, On development of a multi-channel PZT array scanning system  
535 and its evaluating application on UAV wing box, *Sensors and Actuators A:*  
536 *physical*, 151 (2009) 220-230.
- 537 [23] L. Qiu, S. Yuan, X. Zhang, Y. Wang, A time reversal focusing based impact  
538 imaging method and its evaluation on complex composite structures, *Smart Mater.*  
539 *Struct.*, 20 (2011) 105014.
- 540 [24] K. Xu, D. Ta, Z. Su, W. Wang, Transmission analysis of ultrasonic Lamb mode  
541 conversion in a plate with partial-thickness notch, *Ultrasonics*, 54 (2014) 395-401.
- 542 [25] K. Wang, M. Liu, Z. Su, S. Yuan, Z. Fan, Analytical insight into “breathing” crack-  
543 induced acoustic nonlinearity with an application to quantitative evaluation of  
544 contact cracks, *Ultrasonics*, 88 (2018) 157-167.
- 545 [26] K. Wang, Z. Fan, Z. Su, Orienting fatigue cracks using contact acoustic  
546 nonlinearity in scattered plate waves, *Smart Mater. Struct.*, 27 (2018) 09LT01.
- 547 [27] P. Zuo, Z. Fan, SAFE-PML approach for modal study of waveguides with  
548 arbitrary cross sections immersed in inviscid fluid, *J. Sound Vib.*, 406 (2017) 181-  
549 196.
- 550 [28] B. Hilloulin, Y. Zhang, O. Abraham, A. Loukili, F. Grondin, O. Durand, V. Tournat,  
551 Small crack detection in cementitious materials using nonlinear coda wave  
552 modulation, *NDT & E Int.*, 68 (2014) 98-104.
- 553 [29] J.E. Michaels, T.E. Michaels, Detection of structural damage from the local  
554 temporal coherence of diffuse ultrasonic signals, *IEEE Trans. Ultrason. Ferroelectr.*  
555 *Freq. Control*, 52 (2005) 1769-1782.
- 556 [30] Y. Zhang, E. Larose, L. Moreau, G. d’Ozouville, Three-dimensional in-situ  
557 imaging of cracks in concrete using diffuse ultrasound, *Struct. Health Monit.*, 17  
558 (2018) 279-284.
- 559 [31] M. Hong, Z. Su, Y. Lu, H. Sohn, X. Qing, Locating fatigue damage using temporal

560 signal features of nonlinear Lamb waves, *Mech. Syst. Signal Process*, 60 (2015)  
561 182-197.

562 [32] Y. Lu, L. Ye, Z. Su, Crack identification in aluminium plates using Lamb wave  
563 signals of a PZT sensor network, *Smart Mater. Struct.*, 15 (2006) 839.

564 [33] M. Hong, Z. Su, Q. Wang, L. Cheng, X. Qing, Modeling nonlinearities of  
565 ultrasonic waves for fatigue damage characterization: Theory, simulation, and  
566 experimental validation, *Ultrasonics*, 54 (2014) 770-778.

567 [34] Q. Wang, M. Hong, Z. Su, An In-Situ Structural Health Diagnosis Technique and  
568 Its Realization via a Modularized System, *IEEE Trans. Instrum. Meas.*, 64 (2015)  
569 873-887.

570